PLOS ONE

Karyopherin Alpha2 Is Essential for rRNA Transcription and Protein Synthesis in Proliferative Keratinocytes

Noriko Umegaki-Arao[1], Katsuto Tamai[2]*, Keisuke Nimura[3], Satoshi Serada[4], Tetsuji Naka[4], Hajime Nakano[5], Ichiro Katayama[1]

1 Department of Dermatology, Osaka University Graduate School of Medicine, Osaka, Japan, **2** Department of Stem Cell Therapy Science, Osaka University Graduate School of Medicine, Osaka, Japan, **3** Division of Gene Therapy Science, Osaka University Graduate School of Medicine, Osaka, Japan, **4** National Institute of Biomedical Innovation Laboratory for Immune Signal, Osaka, Japan, **5** Department of Dermatology, Hirosaki University School of Medicine, Hirosaki, Japan

Abstract

Karyopherin proteins mediate nucleocytoplasmic trafficking and are critical for protein and RNA subcellular localization. Recent studies suggest KPNA2 expression is induced in tumor cells and is strongly associated with prognosis, although the precise roles and mechanisms of KPNA2 overexpression in proliferative disorders have not been defined. We found that KPNA2 expression is induced in various proliferative disorders of the skin such as psoriasis, Bowen's disease, actinic keratosis, squamous cell carcinoma, Paget's disease, Merkel cell carcinoma, and mycosis fungoides. siRNA-mediated KPNA suppression revealed that KPNA2 is essential for significant suppression of HaCaT proliferation under starvation conditions. Ribosomal RNA transcription and protein synthesis were suppressed by starvation combined with knockdown of KPNA (including KPNA2) expression. KPNA2 localized to the nucleolus and interacted with proteins associated with mRNA processing, ribonucleoprotein complex biogenesis, chromatin modification, and transcription, as demonstrated by tandem affinity purification and mass spectrometry. KPNA2 may be an important promoter of ribosomal RNA and protein synthesis in tumor cells.

Citation: Umegaki-Arao N, Tamai K, Nimura K, Serada S, Naka T, et al. (2013) Karyopherin Alpha2 Is Essential for rRNA Transcription and Protein Synthesis in Proliferative Keratinocytes. PLoS ONE 8(10): e76416. doi:10.1371/journal.pone.0076416

Editor: Andrzej T. Slominski, University of Tennessee, United States of America

Received November 9, 2012; **Accepted** August 29, 2013; **Published** October 3, 2013

Funding: This work was supported by a Grant-in-Aid of Scientific Research from the Ministry of Education, Culture, Science and Technology of Japan, and a Health and Labour Science Research Grant from the Ministry of Health, Labour and Welfare of Japan. The funders had no role in study design, data collection and analysis, decision to publish, or preparation of the manuscript.

Competing Interests: The authors have declared that no competing interests exist.

* E-mail: tamai@gts.med.osaka-u.ac.jp

Introduction

Recent studies have defined the molecular mechanisms of nucleocytoplasmic signal transduction by karyopherins (KPNs), which function as receptors for various intracellular molecules and mediate nuclear import and export during interphase. In humans, the karyopherin alpha (KPNA) family consists of at least 7 family members, all of which interact with karyopherin beta (KPNB) 1 and transport various proteins and RNAs through the nuclear pores in an energy-dependent manner [1–3]. Various extracellular environmental changes activate intracellular signaling cascades by which cells exchange activated signaling molecules between the nucleus and cytoplasm via the KPN-mediated machinery to regulate proliferation and differentiation status [2,4–6]. KPNA2 expression in human epidermal keratinocytes, but not in human dermal fibroblasts, is differentially regulated by transforming growth factor (TGF)-β_1 and interferon (IFN)-γ, both of which are established modulators of epidermal proliferation and differentiation [4]. KPNA2 also mediates the translocation of epidermal differentiation-inducing signals into the nucleus by recruiting transcription factors such as interferon regulatory factor-1 (IRF-1), thereby inducing IFN-γ-mediated epidermal differentiation [4]. Karyopherin alphas also mediate mitotic spindle assembly [7–9] and nuclear membrane formation [10]. KPNB1 is also a global regulator of mitotic spindle assembly, centrosome dynamics, nuclear membrane formation, and nuclear pore complex assembly [11,12]. Recent studies have revealed that KPNs including KPNA2 are overexpressed in various kinds of tumors such as breast cancer, cervical cancer, non-small cell lung cancer, prostate cancer, and primary cutaneous melanoma, and that expression levels in these tumors are closely associated with prognosis [13–18]. Nevertheless, the precise roles and mechanisms of KPN overexpression in proliferative disorders have not been defined.

The rate of cell growth and proliferation is proportional to the rate of protein synthesis, which is tightly linked to ribosome biologics [19,20]. RNA synthesis and ribosome construction occur in the nucleolus and their control is important for regulating protein synthesis; however, the precise mechanisms and roles of karyopherins in regulating rRNA and protein synthesis remain unclear.

We report KPNA2 induction in proliferation disorders regardless of malignancy, and suggest KPNA2 regulates rRNA transcription and general protein synthesis in the nucleolus to maintain proliferation.

Materials and Methods

Skin Samples

Written informed consent was obtained from all patients, and the study protocol was approved by Medical Ethics Committee of Osaka University.

Cell Culture

HaCaT cells, an immortalized, nontumorigenic keratinocyte cell line, were cultured in Dulbecco's modified Eagle's medium (DMEM; Nacalai Tesque) containing 10% fetal bovine serum (FBS) at 37°C under 5% CO_2-95% air.

RNA Purification and Reverse Transcription-quantitative Polymerase Chain Reaction

Total RNA was isolated from HaCaT cells with an RNA isolation kit (Qiagen) and reverse transcribed with SuperScript III reverse transcriptase (Invitrogen). Expression of pre-rRNA was determined by using Power SYBR green PCR Master Mix (Applied Biosystems) according to the manufacturer's protocol. β-Actin was used to normalize target gene expression. PCR amplification was performed with 5′-ATCGTCCACCGCAAATGCTTCTA-3′ and 5′-AGCCATGCCAATCTCATCTTGTT-3′ for β-actin and 5′-GAACGGTGGTGTGTCGTTC-3′ and 5′-GCGTCTCGTCTCGTCTCACT-3′ for pre-rRNA [21]. PCR cycling conditions were 40 cycles of denaturing at 92°C for 15 sec and annealing at 60°C for 60 sec on an ABI Prism 7000 sequence detection system (Applied Biosystems).

Small Interfering RNA and Plasmid DNA Transfection

Small interfering RNAs (siRNAs) specific for KPNA1, 2, 3, and 4 and the control stealth siRNA were obtained from Invitrogen. Cells (1.5×10^6) were transfected with 100 ng siRNAs mixture using the Neon transfection system (Invitrogen). We performed the knockdown studies with each siRNA, which ensured more than 50–70% suppression of KPNA2 mRNA and protein.

MTS

[3-(4,5-dimethylthiazol-2-yl)-5(3-carboxymethoxyphenyl)-2-(4-sulfophenyl)-2H-tetrazolium] assay. HaCaT cells induced with each siRNA were seeded at their optimal cell density (7×10^4 cells/well) in 96-well microtiter plates and incubated to allow cell attachment. After 6 h, cells were incubated with 0.1% FBS DMEM for 24, 48, 72, and 120 h. At the end of each incubation period, cell viability was determined by using the CellTiter 96® AQ_{ueous} Non-Radioactive Cell Proliferation Assay (Promega) according to the manufacturer's instructions. Samples were incubated at 37°C in a humidified 5% CO_2 atmosphere for 1 h. Absorbance was measured at 490 nm using a microplate reader.

Immunohistochemistry

Slides of skin biopsies in paraffin blocks were stained with hematoxylin and eosin (HE) and anti-human KPNA2 mouse monoclonal antibody (BD Biosciences) (1:1000).

Immunofluorescence

HaCaT cells were fixed in 4% formaldehyde in phosphate-buffered saline (PBS) for 40 min. After rinsing twice with PBS, the cells were permeabilized in 0.5% Triton X-100 in PBS for 60 s and blocked with 2% skim milk overnight at 4°C. The cells were incubated with anti-UBF (Santa Cruz) and anti-KPNA2 antibodies for 1 h and stained with Alexa Fluor 546 goat anti-rabbit IgG and Alexa Fluor 488 goat anti-mouse IgG secondary antibodies (1:1000; Invitrogen A-11035 and A-11029) for 1 h. After washing with PBS, cells were counterstained with 0.5 mg/mL 4′, 6′-diamidino-2-phenylindole (DAPI) and mounted with Vectashield mounting medium (Vector Laboratories). Cells were analyzed using a Radiance 2100 confocal scanning-laser microscope (Bio-Rad) equipped with an Eclipse TE-2000 inverted microscope (Nikon) or a Nikon A1 confocal scanning-laser microscope equipped with a Nikon Eclipse Ti inverted microscope.

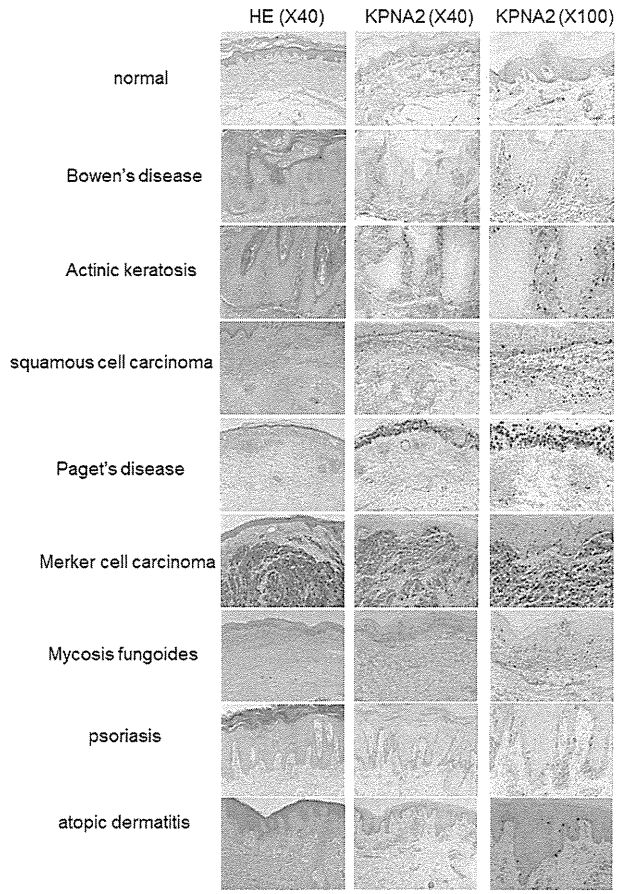

Figure 1. Overexpression of KPNA2 in proliferating cells. Immunohistochemistry showed KPNA2 was uniformly expressed throughout the epidermis in healthy skin, although KPNA2 overexpression was observed in the basal layer in psoriasis. In contrast, very few cells exhibited KPNA2 staining in the basal cells of atopic dermatitis. KPNA2 overexpression was observed in the tumor cells of Bowen's disease, actinic keratosis, squamous cell carcinoma, Paget's disease, Merkel cell carcinoma, and mycosis fungoides.
doi:10.1371/journal.pone.0076416.g001

Tandem Affinity Purification (TAP) and Mass Spectrometry

KPNA2 and GFP cDNAs were introduced into pCAGIP-gw-TAP by using Gateway technology (Invitrogen). KPNA2-TAP and GFP-TAP complexes were purified from HaCaT cell extracts using TAP technology [22,23]. Proteins were separated by SDS-PAGE and stained with the Silver Stain MS Kit (Wako Pure Chemical Industries). Protein bands were excised from the gel and digested with trypsin (Promega) [24]. NanoLC-MS/MS analyses were performed on a LTQ-Orbitrap XL mass spectrometer (Thermo Fisher Scientific) equipped with a nano-ESI source (AMR) and coupled to a Paradigm MG4 pump (Michrom Bioresources) and an autosampler (HTC PAL, CTC Analytics). A spray voltage of 1800 V was applied. The peptide mixture was separated on a MagicC18AQ column (100 μm×150 mm, 3.0 μm particle size, 300 Å, Michrom Bioresources) with a flow rate of 500 nl/min. A linear gradient of 5% to 45% B in 30 min, 45% to 95% B in 0.1 min, and 95% B for 2 min and 5% B was employed

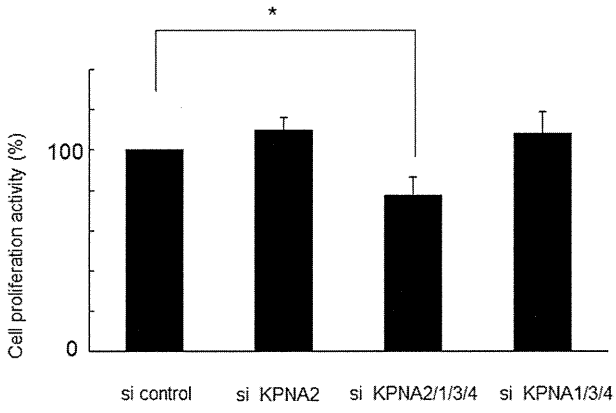

Figure 2. Suppression of cell growth by combined KPNA knockdown. Under starvation conditions (0.1% FBS), siRNA-mediated knockdown of KPNA2, 1, 3, and 4 suppressed cell growth after 120 h (*$p<0.05$). Only KPNA2 siRNA subtraction produced no change in proliferation.
doi:10.1371/journal.pone.0076416.g002

(A = 0.1% formic acid in 2% acetonitrile, B = 0.1% formic acid in 90% acetonitrile). Intact peptides were detected in the Orbitrap at 60,000 resolutions. For LC-MS/MS analysis, 6 precursor ions were selected for MS/MS scans in a data-dependent acquisition mode following each full scan (m/z, 350–1500). A lock mass function was used for the LTQ-Orbitrap to obtain constant mass accuracy during gradient analysis.

Peptides and proteins were identified by automated database searching the Swiss-Prot protein database (version 57.14x) with the MASCOT search program (version 1.0; Matrix Science) and a precursor mass tolerance of 10 p.p.m., a fragment ion mass tolerance of 0.8 Da, and strict trypsin specificity, allowing for up to 2 missed cleavages. Carbamidomethylation of cysteine was set as a fixed modification and oxidation of methionines was allowed as a variable modification.

Metabolic Labeling

HaCaT cells were labeled for 2 h with 100 mCi ^{35}S-methionine in methionine-free DMEM (Gibco) supplemented with 10% dialyzed serum. Protein was extracted with TNE buffer containing 50 mM Tris-HCl at pH 7.4, 150 mM NaCl, 2 mM EDTA, and 0.5% NP-40, then resuspended in 1% sodium dodecyl sulfate and boiled for 10 min at 100°C. Radioactivity was measured with a Beckmann Coulter liquid scintillation counter and normalized to protein content.

Transient Transfection and Luciferase Assay

The human pre-rRNA-luc vector was kindly provided by Dr. Samson Jacob [25]. HaCaT cells induced with each siRNA were seeded in a 12-well plate and transfected with 0.34 μg human-pre-rRNA-luc plasmid and Fugene 6 transfection reagent (Roche). The luciferase reporter assay was performed using a commercial luciferase assay kit (Promega). Data were normalized to the protein concentration.

Statistical Analysis

All data and results were confirmed in at least 3 independent experiments. Statistical significance was determined by one-way analysis of variance (ANOVA).

Results

KPNA2 Overexpression in Proliferative Disorders of the Skin

To investigate KPNA2 expression in various epidermal-proliferative disorders of the skin, immunohistochemical staining of KPNA2 was performed on biopsy specimens of epidermal tumors as well as psoriasis and atopic dermatitis, which are inflammatory skin diseases with higher and lower epidermal proliferation, respectively. KPNA2 staining was faint and homogeneous without significant nuclear accumulation in healthy epidermis. In contrast, there was marked KPNA2 staining in the nuclei and cytoplasm of malignant cells in several skin tumors with different prognoses including Bowen's disease, actinic keratosis, squamous cell carcinoma (SCC), Paget's disease, Merkel cell carcinoma, and Mycosis fungoides. In malignant cells of SCC *in situ* such as Bowen's disease and actinic keratosis as with well prognosis, KPNA2 expressed predominantly in the basal layer. In contrast, established SCC showed rather intense and diffuse expression of KPNA2 in the malignant cells. Non-squamous cell malignant tumors of the skin including Paget's disease, Merkel cell carcinoma, and mycosis fungoides also showed diffuse, intense staining of KPNA2, indicating significantly higher expression in skin malignancy. Marked staining of KPNA2 was also observed in psoriatic skin, but was limited to the cytoplasm of basal layer keratinocytes. In contrast, very few but significant numbers of KPNA2-positive keratinocytes were observed in the basal lesions of atopic dermatitis, particularly in the inflamed proliferating lesions (**Figure 1**).

Contribution of KPNA2 and other KPNAs to Keratinocyte Cell Growth

To assess the role of KPNs in keratinocyte proliferation, HaCaT cell growth in culture was assessed by MTS assay after siRNA-mediated knockdown of KPNs. In culture medium containing 10% FBS, growth was significantly suppressed by KPNB1 knockdown [13]; however, knockdown of other KPNAs produced no significant effect (data not shown). In starved culture medium with 0.1% FBS, HaCaT cell growth was significantly suppressed by siRNA knockdown of KPNA1, 2, 3, and 4, suggesting adequate expression of KPNAs may be required for growth maintenance, especially in starved cells such as cancer cells. About 20% of HaCaT keratinocyte growth was suppressed 120 h after KPNA knockdown. KPNA siRNAs were individually subtracted from the siRNA cocktail to investigate the contribution of each KPNA to growth suppression. Interestingly, only KPNA2 siRNA subtraction resulted in the significant recovery of cell growth up to the control level (**Figure 2**), while removal of the other KPNA siRNAs did not affect growth suppression (data not shown). KPNA2 knockdown alone had no significant growth suppression effect, suggesting the other KPNAs are redundant. These data suggest KPNAs complement each other during cell growth, but KPNA2 may be essential for maintaining cell proliferation under starvation conditions.

Association of KPNA2 with Ribosomal Proteins in the Nucleolus

To identify proteins that interact with KPNA2 in HaCaT keratinocytes, we used the TAP method, which enabled us to easily isolate and purify proteins bound to the stably expressed TAP-tagged target recombinant protein [22,23]. Proteins associated with the KPNA2-TAP complex were isolated from the nuclei and cytoplasm of KPNA2-TAP-expressing HaCaT cells, separated

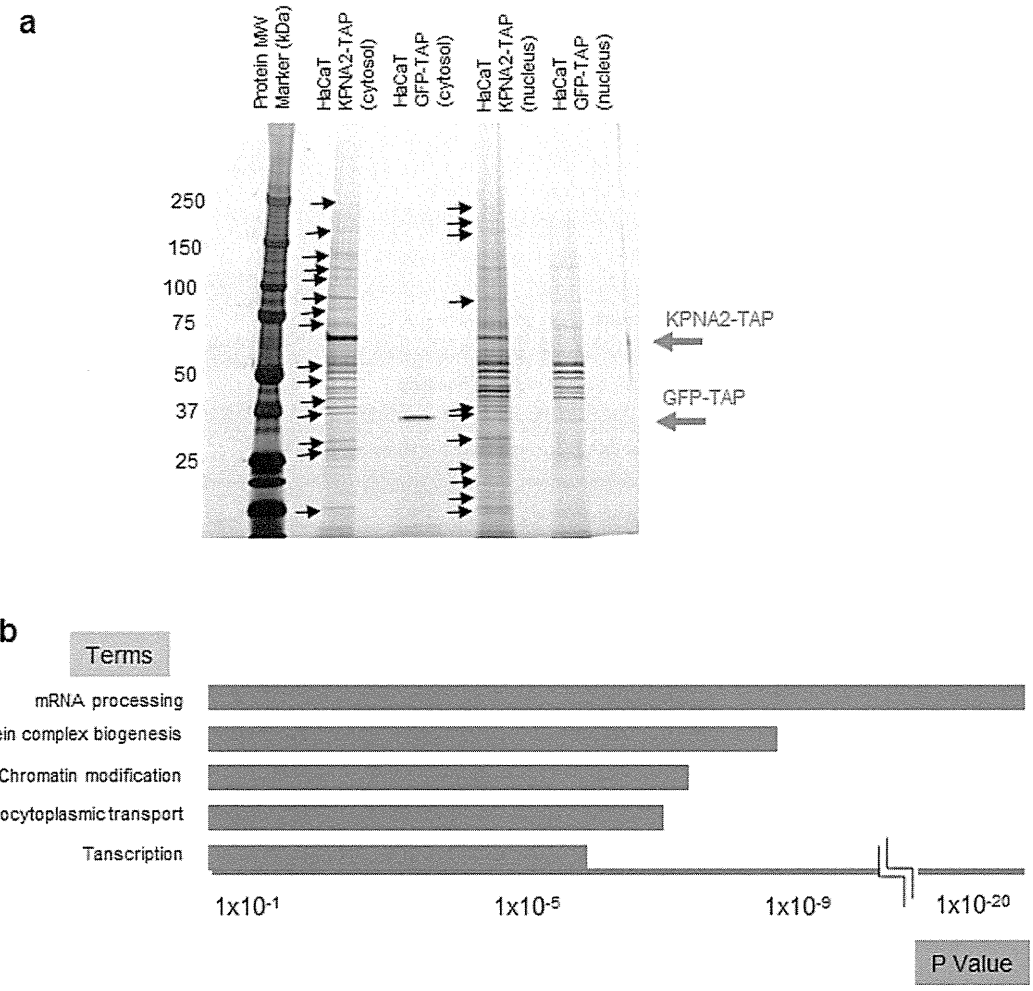

Figure 3. Detection and analysis of proteins that interact with KPNA2 and localization of KPNA2 in the nucleolus. Proteins that interact with KPNA2 in the cytoplasm and nucleus were purified using the TAP method and detected by silver staining. Proteins marked with arrows were analyzed by LC/MS/MS. HaCaT cells expressing GFP-TAP were used to detect nonspecific interactions. **a)** The results of LC/MS/MS were analyzed by pathway analysis using reactome (http://www.reactome.org). The categories of "mRNA processing", "ribonucleoprotein complex biogenesis", "chromatin modification," and "transcription" were the most significantly represented pathways. **b)** Immunohistochemistry revealed KPNA2 co-localization with UBF, a nucleolar marker.
doi:10.1371/journal.pone.0076416.g003

Table 1. Lists of proteins analyzed by pathway analysis.

mRNA processing	
RALY	RNA-binding protein Raly
NCBP1	Nuclear cap-binding protein subunit 1
RNMT	mRNA cap guanine-N7 methyltransferase
GAR1	H/ACA ribonucleoprotein complex subunit 1
PABPC4	PABPC4 protein
MLH1	DNA mismatch repair protein Mlh1
YBX1	Nuclease-sensitive element-binding protein 1
SRRT	Serrate RNA effector molecule homolog
DDX17	Probable ATP-dependent RNA helicase DDX17
RRP1B	Ribosomal RNA processing protein 1 homolog B
PCBP1	Poly(rC)-binding protein 1
PCBP2	Poly(rC)-binding protein 2
SFRS9	Splicing factor, arginine/serine-rich 9
PABPC1	Polyadenylate-binding protein 1
NSUN2	tRNA (cytosine-5-)-methyltransferase NSUN2
KRR1	KRR1 small subunit processome component homolog
DHX9	ATP-dependent RNA helicase A
RRP1	Ribosomal RNA processing protein 1 homolog B
DDX1	ATP-dependent RNA helicase DDX1
HNRNPU	Heterogeneous nuclear ribonucleoprotein U
TTF2	Transcription termination factor 2
SFRS3	Splicing factor, arginine/serine-rich 3
PHAX	Phosphorylated adapter RNA export protein
NOP2	Putative ribosomal RNA methyltransferase NOP2
RPS16	RPS16 protein
SNRNP200	U5 small nuclear ribonucleoprotein 200 kDa helicase
SYF2	Pre-mRNA-splicing factor SYF2
NOP56	NOP56 protein
RBM14	RNA-binding protein 14
BAT1	Spliceosome RNA helicase BAT1
ADAR	Double-stranded RNA-specific adenosine deaminase
KIAA1429	Protein virilizer homolog
Ribonucleoprotein complex biogenesis	
NCBP1	Nuclear cap-binding protein subunit 1
KRR1	KRR1 small subunit processome component homolog
RRP1	Ribosomal RNA processing protein 1 homolog B
GAR1	H/ACA ribonucleoprotein complex subunit 1
NIP7	60 S ribosome subunit biogenesis protein NIP7 homolog
DDX1	ATP-dependent RNA helicase DDX1
PHAX	Phosphorylated adapter RNA export protein
NOP2	Putative ribosomal RNA methyltransferase NOP2
RPS16	RPS16 protein
RRP1B	Ribosomal RNA processing protein 1 homolog B
SNRNP200	U5 small nuclear ribonucleoprotein 200 kDa helicase
SFRS9	Splicing factor, arginine/serine-rich 9
NOP56	NOP56 protein
Chromatin modification	

Table 1. Cont.

mRNA processing	
ING5	Inhibitor of growth protein 5
RBBP4	Histone-binding protein RBBP4
RBBP7	Histone-binding protein RBBP7
ARID2	AT-rich interactive domain-containing protein 2
CHD8	Chromodomain-helicase-DNA-binding protein 8
HDAC2	Histone deacetylase 2
HDAC1	Histone deacetylase 1
ASH1L	Probable histone-lysine N-methyltransferase ASH1L
BRDT	Bromodomain testis-specific protein
RBM14	RNA-binding protein 14
BCOR	BCL-6 corepressor
CHD4	Chromodomain-helicase-DNA-binding protein 4
MLL2	Histone-lysine N-methyltransferase MLL2
Nucleocytoplasmic transport	
PHAX	Phosphorylated adapter RNA export protein
NCBP1	Nuclear cap-binding protein subunit 1
UPF1	Regulator of nonsense transcripts 1
SET	Protein SET
GLE1	Nucleoporin GLE1
NUPL2	Nucleoporin-like protein 2
TPR	Nucleoprotein
KPNA2	Importin subunit alpha-2
KPNB1	Importin subunit beta-1
BAT1	Spliceosome RNA helicase BAT1
Transcription	
ING5	Inhibitor of growth protein 5
NMI	N-myc-interactor
FOXK1	Forkhead box protein K1
FOXM1	Forkhead box protein M1
CCNT1	Cyclin-T1
ARID2	AT-rich interactive domain-containing protein 2
YBX1	Nuclease-sensitive element-binding protein 1
CNOT4	CCR4-NOT transcription complex subunit 4
YBX2	Y-box-binding protein 2
CHD8	Chromodomain-helicase-DNA-binding protein 8
ASH2L	Set1/Ash2 histone methyltransferase complex subunit ASH2
BCOR	BCL-6 corepressor
EWSR1	RNA-binding protein EWS
CHD4	Chromodomain-helicase-DNA-binding protein 4
MLL2	Histone-lysine N-methyltransferase MLL2
ASXL3	Putative Polycomb group protein ASXL3
TAF4	Transcription initiation factor TFIID subunit 4
RBBP4	Histone-binding protein RBBP4
TAF6	Transcription initiation factor TFIID subunit 6
POLR1A	DNA-directed RNA polymerase I subunit RPA1
MED12	Mediator of RNA polymerase II transcription subunit 12
CSDA	DNA-binding protein A

doi:10.1371/journal.pone.0076416.t001

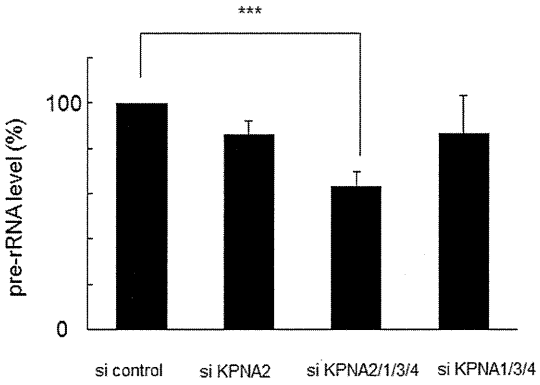

Figure 4. Suppression of ribosomal RNA synthesis by combined KPNA knockdown. Under starvation conditions (0.1% fetal bovine serum), siRNA-mediated knockdown of KPNA2, 1, 3, and 4 significantly suppressed ribosomal RNA synthesis analyzed by reverse transcription-quantitative polymerase chain reaction (***p<0.01). The amount of pre-ribosomal RNA was reduced by about 37% after 72 h.
doi:10.1371/journal.pone.0076416.g004

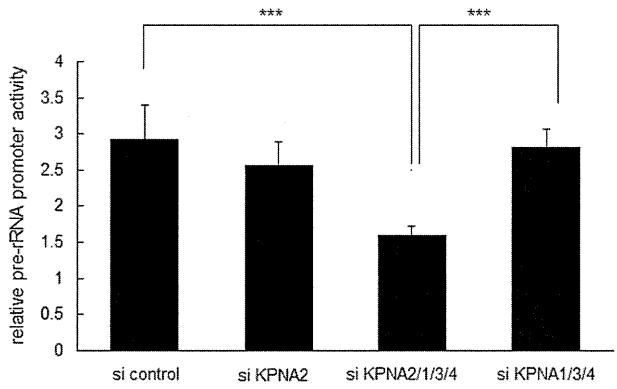

Figure 6. Suppression of the pre-ribosomal RNA promoter by combined KPNA knockdown. Under starvation conditions (0.1% fetal bovine serum), siRNA-mediated knockdown of KPNA2, 1, 3, and 4 significantly suppressed pre-rRNA promoter activity after 24 h (***p<0.01).
doi:10.1371/journal.pone.0076416.g006

by SDS-PAGE, and silver stained. HaCaT cells expressing GFP-TAP were used as a negative control (**Figure 3a**). KPNA2-TAP-associated proteins extracted from the silver-stained gel were identified by mass spectrometry. Numerous proteins were analyzed by reactome (http://www.reactome.org) to investigate their biological relationships. Pathway analysis revealed that the proteins interacting with KPNA2 were associated with mRNA processing, ribonucleoprotein complex biogenesis, chromatin modification, and transcription, all of which are essential for cell activities including cell growth (**Figure 3b, Table 1**). Interestingly, significant numbers of ribosomal proteins were listed as associated with KPNA2. Furthermore, immunofluorescence staining of KPNA2 in cultured HaCaT keratinocytes demonstrated co-localization of KPNA2 with UBF in the nucleoli, suggesting a role of KPNA2 for maintaining rRNA function (**Figure 3c**).

Contribution of KPNA2 to Protein Synthesis and Ribosomal RNA Transcription

Because the nucleolus is specifically responsible for rRNA transcription and maintenance of gene expression/transcription and mRNA processing, we hypothesized that KPNA2 in the nucleoli may regulate rRNA transcription to maintain cell growth under starvation conditions. To test this hypothesis, the siRNA cocktail was again applied to knockdown KPNAs to observe the effect on pre-rRNA transcription in starved HaCaT keratinocytes. Knockdown of all KPNAs reduced pre-rRNA levels as measured by RT-qPCR. In the 72 h after treatment with the siRNA cocktail, pre-rRNA expression was reduced by about 40%. Subtraction of KPNA2 siRNA restored pre-rRNA expression. The other KPNAs did not contribute to pre-rRNA expression. Treatment with KPNA2 siRNA alone had no significant effect, suggesting a redundant mechanism with other KPNAs (**Figure 4**). Protein synthesis in HaCaT keratinocytes was also reduced, corresponding to the suppression of pre-rRNA expression (**Figure 5**). The pre-rRNA promoter was also suppressed by KPNA knockdown after 24 h (**Figure 6**). Fluorescence-activated cell sorting of HaCaT cells before and after KPNA knockdown showed no significant change in the cell cycle pattern (data not shown). These data suggest KPNA2 might positively regulate rRNA transcription in the nucleolus, maintaining cell growth by ensuring transcription and translation directly or indirectly.

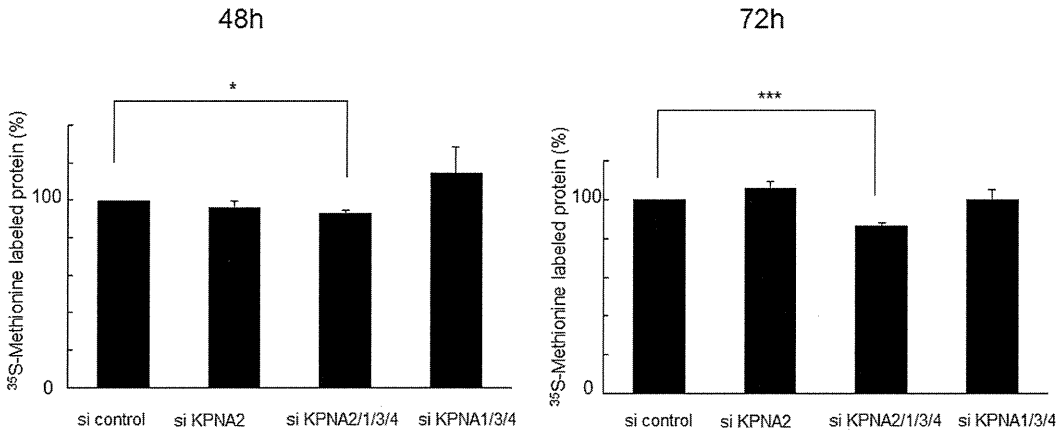

Figure 5. Suppression of protein synthesis by combined KPNA knockdown. Under starvation conditions (0.1% fetal bovine serum), siRNA-mediated knockdown of KPNA2, 1, 3, and 4 significantly suppressed protein synthesis after 48 h (*p<0.05) and 72 h (***p<0.01), as demonstrated by metabolic labeling with ^{35}S-methionine.
doi:10.1371/journal.pone.0076416.g005

Discussion

In this study, KPNA2 was overexpressed in proliferating disorders of the skin and interacted with many kinds of proteins that control transcription and gene expression directly and indirectly. This was the first report to show that KPNA2 is essential for cell growth in terms of rRNA and protein synthesis under starvation conditions.

KPNA2 overexpression in several skin malignancies is associated with varying prognoses. In the basal cells of psoriasis, KPNA2 expression was diffusely up-regulated in comparison to atopic dermatitis. Thus, KPNA2 expression might be induced in cells in which proliferation has been activated. Comparing Bowen's disease and actinic keratosis, which are known as SCC *in situ*, KPNA2 was remarkably and diffusely overexpressed. KPNA2 may therefore be a tumor marker with utility as a prognostic factor of proliferative activity in skin malignancies, although we have insufficient sample sizes to determine significance. Previous reports have demonstrated KPNA2 overexpression in various tumors cells *in vitro* and *in vivo*; elevated KPNA2 and KPNB1 expression in cancer cells correlates with altered transcriptional regulation associated with deregulated E2F/Rb activities [26]. Some studies have indicated that higher KPNA2 expression in tumor cell nuclei shortens patient survival, although the mechanisms and precise roles of KPNA2 in the tumor cells remained unclear [16,17]. Researchers also hypothesized that KPNA2-mediated nuclear transport of proteins necessary for maintaining cell proliferation, such as transcription factors, promote tumor cell growth. In this context, KPNA2 was shown to interact with NBS1 (Nijmegen breakage syndrome 1), a key regulator of the MRE11/RAD50/NBS1 complex. NBS1 promotes tumorigenesis by binding and activating the phosphatidylinositol 3-kinase/AKT pathway [27]. Interestingly, siRNA-medicated KPNA2 knockdown studies revealed a different cellular response to KPNA2 inhibition in prostate and cervical cancer cell lines. In prostate cell line PC3, proliferation and viability were significantly reduced when KPNA2 expression was inhibited, whereas there was no significant change in a cervical cancer cell line. This difference could be due to tissue-specific tumor etiologies [13,17].

In this study, we characterized KPNA2-binding proteins *in situ* in immortalized HaCaT keratinocytes. In silico gene ontology indicated a significant relationship between KPNA2 binding proteins and mRNA processing, ribonucleoprotein complex biogenesis, chromatin modification, and transcription. KPNA2 interacted with various ribosomal proteins and heterogeneous nuclear ribonucleoproteins directly or indirectly and was located in the nucleolus, the site of pre-rRNA transcription and processing and ribosome assembly. rRNA synthesis, the first event in ribosome synthesis, is a fundamental determinant of a cell's capacity to grow and proliferate. Ribosomal RNA genes (rDNAs) are transcribed with high efficiency and the complex regulation of rRNA synthesis is responsive to general metabolism and specific environmental challenges [20,28]. Serum starvation is also a well-established approach to inducing a broad range of cellular stress. TAP analysis revealed that KPNA2 associates with numerous ribosomal RNA synthesis-related proteins including RNA polymerase I subunit, rRNA methyl transferase, rRNA subunit biogenesis protein, and rRNA processing proteins. Furthermore, KPNA2 accumulates in the nucleolus and contributes to rRNA transcription *in vitro*. These lines of evidence suggest KPNA2 may serve important roles as a canonical nuclear transporter and to ensure rRNA biogenesis in proliferating cells. In this context, enhanced KPNA2 expression in malignant and inflammatory keratinocytes may positively regulate their proliferating capacity by supporting rRNA synthesis, which is indispensable. In malignant cells, the poor prognosis indicated by nuclear KPNA2 accumulation may be associated with KPNA2 retention in response to cellular stress and increasing rRNA synthesis or changing gene expression.

KPNA subtypes exhibit different abilities to interact with specific NLS-containing cargos and in various expression patterns in cells and tissues. KPNA2 is highly expressed in undifferentiated embryonic stem cells and down-regulated during neural differentiation, indicating that proper expression of KPNA2 is required for embryonic stem cells to maintain their undifferentiated state [29]. KPNs are also complementary because they are indispensable for cellular proliferation and differentiation. We previously examined the effect of KPNA2 siRNA subtraction on RNA expression in normal human keratinocytes by microarray analysis [4]; however, there was no increases of more than 2 fold in any other KPNs including KPNA1, 3, 4, and KPNB1 (data not shown).

In this study, KPNA2 was essential for cell growth related to rRNA and protein synthesis under starvation conditions; however, there was no significant change when only KPNA2 was knocked down. Combined knockdown of KPNA2, 1, 3, and 4 was needed to suppress cell growth and KPNA2 was indispensable. Even under these conditions, growth suppression was gradual and mild over 120 h. Furthermore, combined knockdown of KPNAs mildly suppressed the synthesis of rRNA and proteins after 72 h. These results indicated that KPNAs might play complementary roles with sufficient reserves.

Further studies are needed to clarify the additional function of KPNA2 in cell proliferation, which would be a focus for a new treatment to regulate KPNA2.

Acknowledgments

We sincerely appreciate the kind support of Prof. Yasufumi Kaneda. We also thank Ms. Eriko Nobuyoshi and Ms. Sayaka Matsumura for technical support with immunohistochemistry and reverse transcription-quantitative polymerase chain reaction.

Author Contributions

Conceived and designed the experiments: NU KT KN TN. Performed the experiments: NU SS. Analyzed the data: NU KT KN TN IK. Contributed reagents/materials/analysis tools: HN IK. Wrote the paper: NU KT.

References

1. Pemberton LF, Paschal BM (2005) Mechanisms of receptor-mediated nuclear import and nuclear export. Traffic 6: 187–198.
2. Yasuhara N, Oka M, Yoneda Y (2009) The role of the nuclear transport system in cell differentiation. Semin Cell Dev Biol 20: 590–599.
3. Yasuda Y, Miyamoto Y, Yamashiro T, Asally M, Masui A, et al. (2012) Nuclear retention of importin alpha coordinates cell fate through changes in gene expression. EMBO J 31: 83–94.
4. Umegaki N, Tamai K, Nakano H, Moritsugu R, Yamazaki T, et al. (2007) Differential regulation of karyopherin alpha 2 expression by TGF-beta1 and IFN-gamma in normal human epidermal keratinocytes: evident contribution of KPNA2 for nuclear translocation of IRF-1. J Invest Dermatol 127: 1456–1464.
5. Freire J, Covelo G, Sarandeses C, Diaz-Jullien C, Freire M (2001) Identification of nuclear-import and cell-cycle regulatory proteins that bind to prothymosin alpha. Biochem Cell Biol 79: 123–131.
6. Hall MN, Griffin CA, Simionescu A, Corbett AH, Pavlath GK (2011) Distinct roles for classical nuclear import receptors in the growth of multinucleated muscle cells. Dev Biol 357: 248–258.
7. Schatz CA, Santarella R, Hoenger A, Karsenti E, Mattaj IW, et al. (2003) Importin alpha-regulated nucleation of microtubules by TPX2. EMBO J 22: 2060–2070.

8. Gruss OJ, Carazo-Salas RE, Schatz CA, Guarguaglini G, Kast J, et al. (2001) Ran induces spindle assembly by reversing the inhibitory effect of importin alpha on TPX2 activity. Cell 104: 83–93.
9. Ems-McClung SC, Zheng Y, Walczak CE (2004) Importin alpha/beta and Ran-GTP regulate XCTK2 microtubule binding through a bipartite nuclear localization signal. Mol Biol Cell 15: 46–57.
10. Askjaer P, Galy V, Hannak E, Mattaj IW (2002) Ran GTPase cycle and importins alpha and beta are essential for spindle formation and nuclear envelope assembly in living Caenorhabditis elegans embryos. Mol Biol Cell 13: 4355–4370.
11. Harel A, Forbes DJ (2004) Importin beta: conducting a much larger cellular symphony. Mol Cell 16: 319–330.
12. Rotem A, Gruber R, Shorer H, Shaulov L, Klein E, et al. (2009) Importin beta regulates the seeding of chromatin with initiation sites for nuclear pore assembly. Mol Biol Cell 20: 4031–4042.
13. van der Watt PJ, Maske CP, Hendricks DT, Parker MI, Denny L, et al. (2009) The Karyopherin proteins, Crm1 and Karyopherin beta1, are overexpressed in cervical cancer and are critical for cancer cell survival and proliferation. Int J Cancer 124: 1829–1840.
14. Winnepenninckx V, Lazar V, Michiels S, Dessen P, Stas M, et al. (2006) Gene expression profiling of primary cutaneous melanoma and clinical outcome. J Natl Cancer Inst 98: 472–482.
15. Wang CI, Wang CL, Wang CW, Chen CD, Wu CC, et al. (2011) Importin subunit alpha-2 is identified as a potential biomarker for non-small cell lung cancer by integration of the cancer cell secretome and tissue transcriptome. Int J Cancer 128: 2364–2372.
16. Gluz O, Wild P, Meiler R, Diallo-Danebrock R, Ting E, et al. (2008) Nuclear karyopherin alpha2 expression predicts poor survival in patients with advanced breast cancer irrespective of treatment intensity. Int J Cancer 123: 1433–1438.
17. Mortezavi A, Hermanns T, Seifert HH, Baumgartner MK, Provenzano M, et al. (2011) KPNA2 expression is an independent adverse predictor of biochemical recurrence after radical prostatectomy. Clin Cancer Res 17: 1111–1121.
18. Noetzel E, Rose M, Bornemann J, Gajewski M, Knuchel R, et al. (2012) Nuclear transport receptor karyopherin-alpha2 promotes malignant breast cancer phenotypes in vitro. Oncogene 31: 2101–2114.
19. Tanaka Y, Okamoto K, Teye K, Umata T, Yamagiwa N, et al. (2010) JmjC enzyme KDM2A is a regulator of rRNA transcription in response to starvation. EMBO J 29: 1510–1522.
20. Grummt I (2003) Life on a planet of its own: regulation of RNA polymerase I transcription in the nucleolus. Genes Dev 17: 1691–1702.
21. Murayama A, Ohmori K, Fujimura A, Minami H, Yasuzawa-Tanaka K, et al. (2008) Epigenetic control of rDNA loci in response to intracellular energy status. Cell 133: 627–639.
22. Rigaut G, Shevchenko A, Rutz B, Wilm M, Mann M, et al. (1999) A generic protein purification method for protein complex characterization and proteome exploration. Nat Biotechnol 17: 1030–1032.
23. Nimura K, Ura K, Shiratori H, Ikawa M, Okabe M, et al. (2009) A histone H3 lysine 36 trimethyltransferase links Nkx2–5 to Wolf-Hirschhorn syndrome. Nature 460: 287–291.
24. Shevchenko A, Wilm M, Vorm O, Mann M (1996) Mass spectrometric sequencing of proteins silver-stained polyacrylamide gels. Anal Chem 68: 850–858.
25. Ghoshal K, Majumder S, Datta J, Motiwala T, Bai S, et al. (2004) Role of human ribosomal RNA (rRNA) promoter methylation and of methyl-CpG-binding protein MBD2 in the suppression of rRNA gene expression. J Biol Chem 279: 6783–6793.
26. van der Watt PJ, Ngarande E, Leaner VD (2011) Overexpression of Kpnbeta1 and Kpnalpha2 importin proteins in cancer derives from deregulated E2F activity. PLoS One 6: e27723.
27. Teng SC, Wu KJ, Tseng SF, Wong CW, Kao L (2006) Importin KPNA2, NBS1, DNA repair and tumorigenesis. J Mol Histol 37: 293–299.
28. Moss T (2004) At the crossroads of growth control; making ribosomal RNA. Curr Opin Genet Dev 14: 210–217.
29. Yasuhara N, Shibazaki N, Tanaka S, Nagai M, Kamikawa Y, et al. (2007) Triggering neural differentiation of ES cells by subtype switching of importin-alpha. Nat Cell Biol 9: 72–79.

Evaluation of intramitochondrial ATP levels identifies G0/G1 switch gene 2 as a positive regulator of oxidative phosphorylation

Hidetaka Kioka[a,b,1], Hisakazu Kato[a,1], Makoto Fujikawa[c], Osamu Tsukamoto[a], Toshiharu Suzuki[d,e], Hiromi Imamura[f], Atsushi Nakano[a,g], Shuichiro Higo[a,b], Satoru Yamazaki[h], Takashi Matsuzaki[b], Kazuaki Takafuji[i], Hiroshi Asanuma[j], Masanori Asakura[g], Tetsuo Minamino[b], Yasunori Shintani[a], Masasuke Yoshida[e], Hiroyuki Noji[k], Masafumi Kitakaze[g], Issei Komuro[b,l], Yoshihiro Asano[a,b,2], and Seiji Takashima[a,2]

Departments of [a]Medical Biochemistry and [b]Cardiovascular Medicine and [i]Center for Research Education, Osaka University Graduate School of Medicine, Osaka 565-0871, Japan; [c]Department of Biochemistry, Faculty of Pharmaceutical Science, Tokyo University of Science, Chiba 278-8510, Japan; [d]Chemical Resources Laboratory, Tokyo Institute of Technology, Yokohama 226-8503, Japan; [e]Department of Molecular Bioscience, Kyoto Sangyo University, Kyoto 603-8555, Japan; [f]The Hakubi Center for Advanced Research and Graduate School of Biostudies, Kyoto University, Kyoto 606-8501, Japan; Departments of [g]Clinical Research and Development and [h]Cell Biology, National Cerebral and Cardiovascular Center Research Institute, Osaka 565-8565, Japan; [j]Department of Cardiovascular Science and Technology, Kyoto Prefectural University School of Medicine, Kyoto 602-8566, Japan; and [k]Department of Applied Chemistry, School of Engineering and [l]Department of Cardiovascular Medicine, Graduate School of Medicine, University of Tokyo, Tokyo 113-8656, Japan

Edited by Gottfried Schatz, University of Basel, Reinach, Switzerland, and approved November 19, 2013 (received for review October 7, 2013)

The oxidative phosphorylation (OXPHOS) system generates most of the ATP in respiring cells. ATP-depleting conditions, such as hypoxia, trigger responses that promote ATP production. However, how OXPHOS is regulated during hypoxia has yet to be elucidated. In this study, selective measurement of intramitochondrial ATP levels identified the hypoxia-inducible protein G0/G1 switch gene 2 (G0s2) as a positive regulator of OXPHOS. A mitochondria-targeted, FRET-based ATP biosensor enabled us to assess OXPHOS activity in living cells. Mitochondria-targeted, FRET-based ATP biosensor and ATP production assay in a semi-intact cell system revealed that G0s2 increases mitochondrial ATP production. The expression of G0s2 was rapidly and transiently induced by hypoxic stimuli, and G0s2 interacts with OXPHOS complex V (F_oF_1-ATP synthase). Furthermore, physiological enhancement of G0s2 expression prevented cells from ATP depletion and induced a cellular tolerance for hypoxic stress. These results show that G0s2 positively regulates OXPHOS activity by interacting with F_oF_1-ATP synthase, which causes an increase in ATP production in response to hypoxic stress and protects cells from a critical energy crisis. These findings contribute to the understanding of a unique stress response to energy depletion. Additionally, this study shows the importance of assessing intramitochondrial ATP levels to evaluate OXPHOS activity in living cells.

energy metabolism | live-cell imaging

Maintaining cellular homeostasis and activities requires a stable energy supply. Most eukaryotic cells generate ATP as their energy currency mainly through the mitochondrial oxidative phosphorylation (OXPHOS) system. The OXPHOS system consists of five large protein complex units (i.e., complexes I–V), comprising more than 100 proteins. In this system, oxygen (O_2) is essential as the terminal electron acceptor for complex IV to finally produce the proton-motive force that drives the ATP-generating molecular motor complex V (F_oF_1-ATP synthase).

Hypoxia causes the depletion of intracellular ATP and triggers adaptive cellular responses to help maintain intracellular ATP levels and minimize any deleterious effects of energy depletion. Although the metabolic switch from mitochondrial respiration to anaerobic glycolysis is widely recognized (1–4), several recent reports have shown that hypoxic stimuli unexpectedly increase OXPHOS efficiency as well (5–7). In other words, cells have adaptive mechanisms to maintain intracellular ATP levels by enhancing OXPHOS, particularly in the early phase of hypoxia, in which the O_2 supply is limited but still remains. However, the mechanism by which OXPHOS is regulated during this early hypoxic phase is still not fully understood.

Revealing the mechanism of this fine-tuned regulation of OXPHOS requires accurate and noninvasive measurements of OXPHOS activity. Although researchers have established methods to measure OXPHOS activity, precise measurement, especially in living cells, is still difficult. Measuring the intracellular ATP concentration is one of the most commonly used methods for evaluating OXPHOS activity. However, there are two major problems with this method. First, the intracellular ATP concentration does not always accurately reflect OXPHOS activity, because it can also be affected by glycolytic ATP production, cytosolic ATPases, and ATP buffering enzymes, such as creatine kinase and adenylate kinase (8). Second, because measurements of the ATP concentration by chromatography (9), MS (10), NMR (11), or luciferase assays (12) are based on cell extract analysis, these methods cannot be used to measure the serial ATP concentration changes in living cells in real time.

In this study, we overcame these problems by the selective measurement of the intramitochondrial matrix ATP concentration ($[ATP]_{mito}$) in living cells. In the final step of OXPHOS, ATP is produced not in the cytosol but in the mitochondrial matrix. Therefore, we hypothesized that a selectively measuring $[ATP]_{mito}$ is suitable for the highly sensitive evaluation of cellular ATP production by OXPHOS. In fact, real-time evaluation of both $[ATP]_{mito}$ and the cytosolic ATP concentration ($[ATP]_{cyto}$) in living cells revealed that $[ATP]_{mito}$ reflected OXPHOS activity with far more sensitivity than $[ATP]_{cyto}$. Using this fine method, we found that G0/G1 switch gene 2 (G0s2), a hypoxia-induced

Significance

We developed a sensitive method to assess the activity of oxidative phosphorylation in living cells using a FRET-based ATP biosensor. We then revealed that G0/G1 switch gene 2, a protein rapidly induced by hypoxia, increases mitochondrial ATP production by interacting with F_oF_1-ATP synthase and protects cells from a critical energy crisis.

Author contributions: Y.A. and S.T. designed research; H. Kioka, H. Kato, O.T., and A.N. performed research; M.F., T.S., H.I., S.H., S.Y., T. Matsuzaki, K.T., H.A., M.A., T. Minamino, Y.S., M.Y., H.N., M.K., and I.K. contributed new reagents/analytic tools; H. Kioka and H. Kato analyzed data; and Y.A. and S.T. wrote the paper.

The authors declare no conflict of interest.

This article is a PNAS Direct Submission.

[1]H. Kioka and H. Kato contributed equally to this work.

[2]To whom correspondence may be addressed. E-mail: asano@cardiology.med.osaka-u.ac.jp or takasima@cardiology.med.osaka-u.ac.jp.

This article contains supporting information online at www.pnas.org/lookup/suppl/doi:10.1073/pnas.1318547111/-/DCSupplemental.

protein in cardiomyocytes, increases OXPHOS activity. G0s2 interacted with F_oF_1-ATP synthase and increased the ATP production rate. Our results suggest that hypoxia-induced protein G0s2 is a positive regulator of OXPHOS and protects cells by preserving ATP production, even under hypoxic conditions.

Results

Establishment of a Sensitive Method to Assess OXPHOS Activity in Living Cells. To elucidate the mechanism by which OXPHOS is regulated under hypoxia, it is essential to establish a sensitive method for assessing OXPHOS activity in living cells. For this purpose, we used an ATP indicator based on ε-subunit for analytical measurements (ATeam), which is an ATP-sensing FRET-based indicator (13). We introduced this ATP biosensor into cardiomyocytes that possess an abundance of mitochondria and produce the highest levels of ATP among all primary cells (14, 15). The ATeam assay can measure both $[ATP]_{cyto}$ (i.e., the Cyto-ATeam assay) and $[ATP]_{mito}$ when a duplex of the mitochondrial targeting signal of cytochrome *c* oxidase subunit VIII is attached to the indicator (i.e., the Mit-ATeam assay). In this case, the YFP/CFP emission ratio of the ATeam fluorescence represents the ATP concentration in each compartment. Interestingly, the Mit-ATeam assay was a far more sensitive method than the Cyto-ATeam assay in determining OXPHOS activity in living cells. For example, a very low dose of oligomycin A (0.01 μg/mL), a specific OXPHOS complex V (F_oF_1-ATP synthase) inhibitor, greatly reduced the YFP/CFP emission ratio of the Mit-ATeam fluorescence that represents $[ATP]_{mito}$ within 10 min (Fig. 1 *A*, *Upper* and *B* and Movie S1). In contrast, the same dose of oligomycin A resulted in a slight and slow decline of the YFP/CFP emission ratio of Cyto-ATeam fluorescence (Fig. 1 *A*, *Lower* and *B* and Movie S1). The same phenomenon was observed when the cells were exposed to hypoxia, which suppresses the activity of OXPHOS complex IV (cytochrome *c* oxidase). Again, $[ATP]_{mito}$ decreased more markedly than $[ATP]_{cyto}$ during 2.5 h of hypoxia (Fig. 1 *C* and *D* and Movie S2). These results indicate that the Mit-ATeam assay is far more sensitive for measuring the activity of OXPHOS than the Cyto-ATeam assay. In addition, OXPHOS inhibition decreased the YFP/CFP emission ratio of the Mit-ATeam fluorescence of HeLa cells as well as cardiomyocytes (Fig. S1), suggesting the broad applicability of this assay. Therefore, we used Mit-ATeam for the assessment of the OXPHOS activity in living cells.

Hypoxia-Induced Gene G0s2 Affects the Intramitochondrial ATP Concentration. The expression of genes involved in OXPHOS regulation is considered to be up-regulated in the early phase of hypoxia. Thus, to find unique OXPHOS regulators, we focused on the rapidly induced genes in response to hypoxic stimulation. We compared the gene expression profiles of cultured rat cardiomyocytes at three different time points during hypoxic conditions (0, 2, and 12 h) (Fig. S2*A*). The expression of well-known hypoxia-induced genes, such as VEGF-α and hexokinase 2 mRNA (16, 17), was slightly up-regulated at 2 h and further enhanced at 12 h of hypoxia. In contrast, three other genes (*Adamts1*, *Cdkn3*, and *G0s2*) underwent rapid increases in expression at 2 h but declined at 12 h of sustained hypoxia (Fig. S2 *B* and *C*). This rapid and transient time course of expression implies that these three genes may play distinct regulatory roles, especially in the early hypoxic phase, in which oxygen is limited but still available. To examine whether these genes are involved in the regulation of OXPHOS activity, we knocked down these genes by shRNA (see Fig. S7*A*) and examined $[ATP]_{mito}$ using the Mit-ATeam assay. In this experiment, $[ATP]_{mito}$ in cardiomyocytes treated with shRNA for G0s2 clearly declined within 24 h compared with the control cardiomyocytes (Fig. 2*A* and Movie S3). In addition, the time course of ATP decline was in agreement with the time course of G0s2 depletion (Fig. 2*A* and Fig. S3*A*). Importantly, the overexpression of G0s2 restored normal ATP levels (Fig. 2 *B* and *C*), and again, the Cyto-ATeam assay could not detect a significant effect of G0s2 knockdown within this time frame (Fig. S3*B* and Movie S4). These findings imply that mitochondrial ATP production through OXPHOS was inhibited by G0s2 ablation. We confirmed that the mRNA and protein levels of G0s2 both increased after 2–6 h of hypoxia and then declined after 12 h of hypoxia (Fig. 2 *D* and *E*). G0s2 was first reported as a gene with

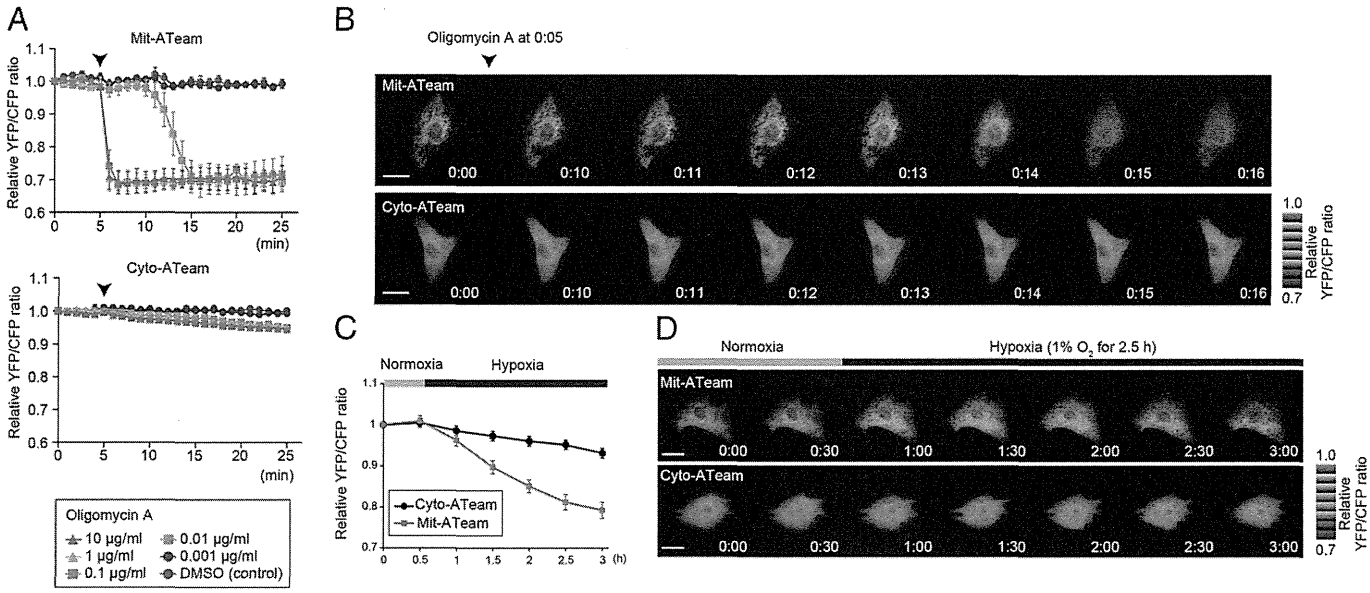

Fig. 1. Establishment of a sensitive method to assess OXPHOS activity in living cells. (*A*) YFP/CFP emission ratio plots of (*Upper*) Mit-ATeam and (*Lower*) Cyto-ATeam fluorescence in cardiomyocytes. Various concentrations (0.001, 0.01, 0.1, 1, and 10 μg/mL) of oligomycin A or DMSO (control) were added at 5 min (arrowhead; $n = 3$). (*B*) Representative sequential YFP/CFP ratiometric pseudocolored images of (*Upper*) Mit-ATeam and (*Lower*) Cyto-ATeam in cardiomyocytes. Oligomycin A (0.01 μg/mL) was added at 5 min. (Scale bars: 20 μm.) (*C*) YFP/CFP emission ratio plots of Mit-ATeam and Cyto-ATeam fluorescence in cardiomyocytes ($n = 10$). (*D*) Representative sequential YFP/CFP ratiometric pseudocolored images of (*Upper*) Mit-ATeam and (*Lower*) Cyto-ATeam in cardiomyocytes. Cells were exposed to 1% hypoxia from the time point 30 min. All of the measurements were normalized to the YFP/CFP emission ratio at 0 min. Data are represented as the means ± SEMs. (Scale bars: 20 μm.)

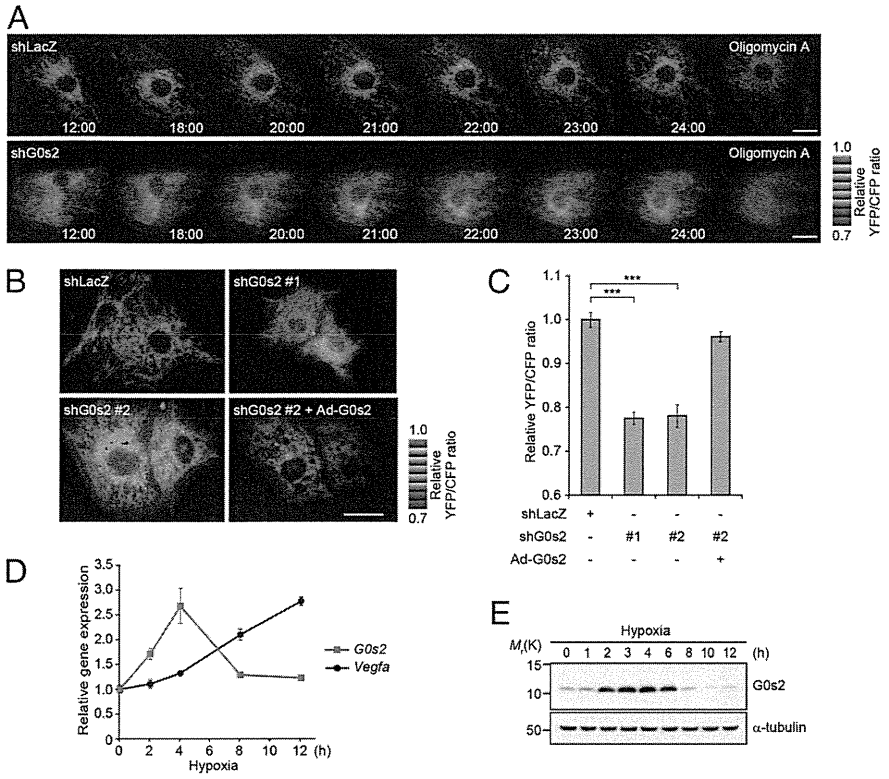

Fig. 2. G0s2, a hypoxia-inducible protein, affects intramitochondrial ATP concentration in cardiomyocytes. (*A*) Sequential YFP/CFP ratiometric pseudocolored images of Mit-ATeam fluorescence in cardiomyocytes expressing (*Upper*) shRNAs for LacZ (shLacZ) or (*Lower*) G0s2 (shG0s2). Oligomycin A (1 μg/mL) was added at the end of the time-lapse imaging to completely inhibit ATP synthesis. The indicated time represents the period after adenovirus infection. (*B*) Representative YFP/CFP ratiometric pseudocolored images of Mit-ATeam fluorescence in cardiomyocytes expressing the indicated adenovirus for 24 h. (Scale bar: *A* and *B*, 20 μm.) (*C*) The bar graph shows the mean YFP/CFP emission ratio of Mit-ATeam fluorescence in cardiomyocytes expressing shLacZ (n = 30), shG0s2 #1 (n = 30), shG0s2 #2 (n = 29), and shG0s2 #2 + G0s2 WT (n = 32) for 24 h. All of the measurements were normalized to the average of the control cells (shLacZ). ***$P < 0.001$. (*D*) Gene expression value plots of *G0s2* (red line) and *VEGF-α* (*Vegfa*; black line) levels in cardiomyocytes under hypoxic conditions (1% O_2). Each value was compared with the level of *Actb* expression (n = 3). Values represent the means ± SEMs. (*E*) Immunoblotting of the G0s2 expression in cardiomyocytes under hypoxic conditions (1% O_2).

expression that was induced during the cell cycle switch from G0 to G1 phase (18). G0s2 is expressed in many tissues and especially abundant in heart, skeletal muscle, liver, kidney, brain, and adipose tissue (19). Although G0s2 may play a role in cell cycle progression (20), the function of G0s2 in the hypoxic response remains unknown.

G0s2 Rescues the Decline of ATP Production During Hypoxia. We next tested whether the overexpression of the G0s2 before hypoxic stress could prevent hypoxia-induced ATP depletion. We prepared cardiomyocytes overexpressing G0s2 and control cardiomyocytes. During sustained hypoxia, $[ATP]_{mito}$ gradually declined in control cardiomyocytes as measured by the Mit-ATeam assay. Notably, the overexpression of G0s2 before the onset of hypoxia reduced this decline in $[ATP]_{mito}$, which allowed the cardiomyocytes to promptly recover to baseline levels of $[ATP]_{mito}$ after reoxygenation (Fig. 3 *A* and *B* and Movie S5). In addition, the prehypoxia overexpression of G0s2 preserved cell viability during sustained hypoxia (Fig. 3*C*). These results suggest that G0s2 can preserve mitochondrial ATP production even under hypoxia and protect cells from the energy crisis under hypoxia.

G0s2 Binds to F_oF_1-ATP Synthase but Not Other OXPHOS Protein Complexes. To reveal the mechanism by which G0s2 affects $[ATP]_{mito}$, we sought to identify the biochemical targets of G0s2. We screened for G0s2 binding proteins by immunoaffinity purification of cell lysates from cardiomyocytes expressing C-terminally Flag-tagged G0s2 (G0s2-Flag). G0s2-Flag is expressed in cardiomyocytes localized to the mitochondria (Fig. S4*A*). MS analysis revealed that multiple F_oF_1-ATP synthase subunits, but no other mitochondrial respiratory chain complex subunits, were coimmunoprecipitated with G0s2-Flag (Fig. S4*B* and Table S1). F_oF_1-ATP synthase is a well-known ATP-producing enzyme composed of a protein complex that contains an extramembranous F_1 and an intramembranous F_o domain linked by a peripheral and a central stalk (21–24). The binding of F_oF_1-ATP synthase to G0s2-Flag was confirmed by immunoblotting with antibodies against several subunits of F_oF_1-ATP synthase (Fig. 4*A*).

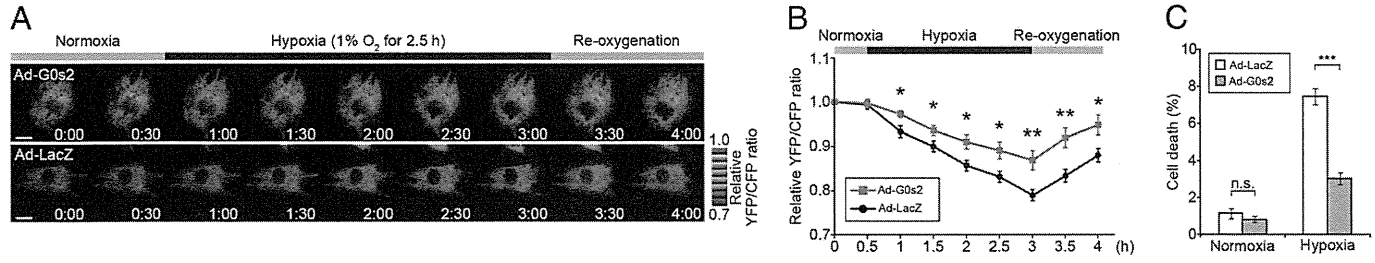

Fig. 3. Overexpression of G0s2 before hypoxia rescues the decline of mitochondrial ATP production during hypoxia. (*A*) Sequential YFP/CFP ratiometric pseudocolored images of Mit-ATeam fluorescence in cardiomyocytes expressing (*Upper*) G0s2 WT or (*Lower*) LacZ during hypoxia and reoxygenation. (Scale bar: 20 μm.) (*B*) YFP/CFP emission ratio plots of Mit-ATeam fluorescence in cardiomyocytes expressing G0s2 WT (n = 20) or LacZ (n = 19) during hypoxia and reoxygenation. All of the measurements were normalized to the ratio at time 0 and compared between cardiomyocytes with G0s2 WT and LacZ at each time point. (*C*) The bar graph shows the cell viability of cardiomyocytes overexpressing G0s2 under hypoxic conditions. Cardiomyocytes expressing either LacZ or G0s2 WT were cultured under normoxic or hypoxic conditions for 18 h (n = 8). The asterisks denote statistical significance comparing G0s2 with LacZ. Data are represented as the means ± SEMs. n.s., not significant. *$P < 0.05$; **$P < 0.01$; ***$P < 0.001$.

Conversely, G0s2-Flag was coimmunoprecipitated with F_oF_1-ATP synthase (Fig. S4*C*). G0s2-Flag was also found to be associated with the F_oF_1-ATP synthase in 293T and HeLa cells (Fig. S4*C*). Both coimmunoprecipitation using an anti-G0s2 antibody and a reciprocal immunoprecipitation revealed that endogenous G0s2 interacts with F_oF_1-ATP synthase, whereas none of the proteins in complexes I–IV or adenine nucleotide translocase 1 (ANT1; also referred to as ADP/ATP carrier) were coimmunoprecipitated with G0s2 (Fig. 4 *B* and *C*).

Given that the G0s2 protein contains an evolutionarily conserved amino terminus and one hydrophobic domain (HD) (19), we created three G0s2 partial deletion mutants to identify the domain in G0s2 that is important for binding to F_oF_1-ATP synthase (Fig. S4*D*). Among these mutants, G0s2 ΔC and G0s2 ΔN but not G0s2 ΔHD bound to the F_oF_1-ATP synthase complex (Fig. 4*D* and Fig. S4 *E* and *F*). Furthermore, we confirmed that G0s2 directly interacts with F_oF_1-ATP synthase in an in vitro pull-down assay using a recombinant maltose-binding protein–fused G0s2 protein and purified F_oF_1-ATP synthase from bovine heart mitochondria (Fig. S5). Immunocytochemical analysis revealed that endogenous G0s2 colocalized with the β-subunit of F_oF_1-ATP synthase (Fig. 4*E*). The knockdown of G0s2 expression by shRNA abolished G0s2 staining (Figs. S6 and S7*A*), indicating that both antibodies used for immunostaining specifically recognize G0s2. These data suggest that G0s2 interacts with the F_oF_1-ATP synthase complex through its HD in mitochondria and regulates OXPHOS activity.

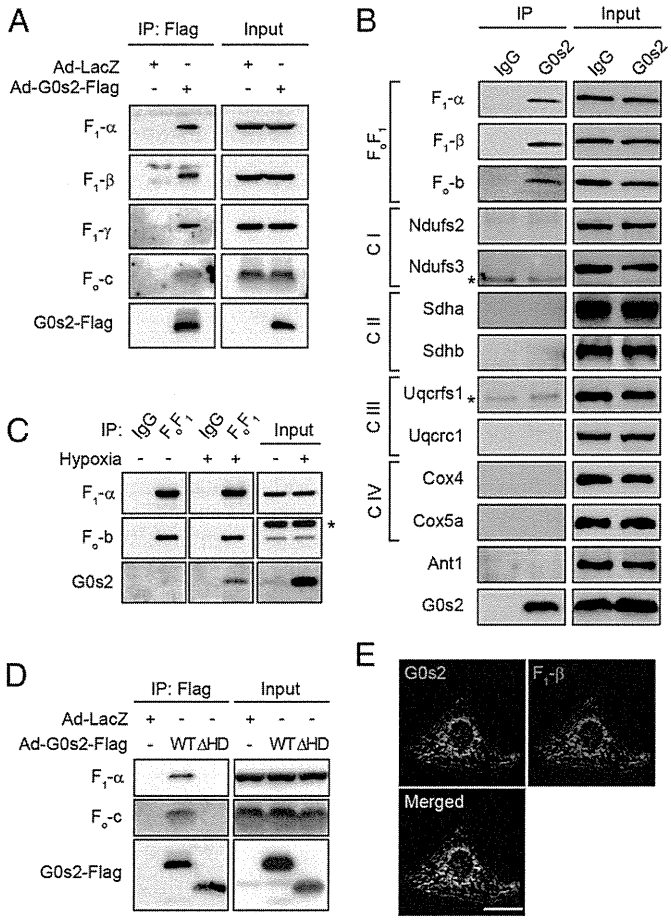

Fig. 4. G0s2 interacts with the F_oF_1-ATP synthase in mitochondria. (*A*) Immunoprecipitation (IP) of G0s2-Flag in cardiomyocytes. Cell lysates from cardiomyocytes expressing G0s2-Flag or LacZ were immunoprecipitated with an anti-Flag antibody. (*B*) IP of endogenous G0s2 in cardiomyocytes. Endogenous G0s2 was induced by hypoxia and immunoprecipitated using an anti-G0s2 antibody. C, OXPHOS complex; F_oF_1, F_oF_1-ATP synthase. *IgG light chain. (*C*) IP of F_oF_1-ATP synthase in cardiomyocytes under normoxic or hypoxic conditions. Cell lysates from cardiomyocytes cultured under normoxia or hypoxia for 4 h were immunoprecipitated with an antibody against the whole F_oF_1-ATP synthase complex or a control IgG. *Nonspecific band. (*D*) IP of G0s2 mutants expressed in cardiomyocytes. Cell lysates were immunoprecipitated with an anti-Flag antibody. (*E*) Immunostained images of hypoxia-stimulated (4 h) cardiomyocytes with anti-G0s2 (green) and anti–F_oF_1-ATP synthase β-subunit (red) antibodies. (Scale bars: 20 μm.)

G0s2 Increases Mitochondrial ATP Production Rate. $[ATP]_{mito}$ is mainly determined by the rate of ATP synthesis by F_oF_1-ATP synthase and ATP/ADP exchange by the ATP/ADP translocase ANT1. This theory means that the increased $[ATP]_{mito}$ observed in the G0s2-overexpressing cells may result from the increased ATP synthesis and/or decreased ATP/ADP exchange, although G0s2 did not interact with ANT1 (Fig. 4*B*). To resolve this issue and directly measure the rate of ATP production in mitochondria, we used a semiintact cell system called the mitochondrial activity of streptolysin O permeabilized cells (MASC) assay (25). In this assay, we permeabilized the plasma membrane to wash out any cytosolic components, such as creatine and glycolytic substrates, but left the mitochondria intact. Furthermore, we treated the cells with P^1, P^5-di(adenosine-5′) pentaphosphate to inhibit the activity of adenylate kinase. These steps allowed us to measure the ATP production rate mostly from OXPHOS, with a minimal contribution of ATP buffering systems in the cytosol. The MASC assay was suitable for accurate measurement of mitochondrial ATP production rate, because mitochondria in this semiintact cell system suffered much smaller damage than the isolated mitochondria in the conventional method. Surprisingly, in the MASC assay, the ATP production rate markedly increased when G0s2 was expressed in HeLa cells that lacked endogenous G0s2 (Fig. 5*A*). In cardiomyocytes, shRNA-mediated G0s2 knockdown decreased the ATP production rate in mitochondria, and the expression of G0s2 WT but not G0s2 ΔHD could restore the ATP production rate (Fig. 5*B* and Fig. S7*A*). In both cells, complete inhibition of ATP production by oligomycin A indicated that the observed ATP synthesis was catalyzed by OXPHOS but not other metabolism (Fig. 5 *A* and *B*).

Next, to evaluate the physiological role of G0s2, we examined whether endogenous G0s2 induced by hypoxia could enhance the ATP production rate. Cardiomyocytes were pretreated with hypoxia for 4 h, during which G0s2 expression was largely induced. We then evaluated the ATP production rate of both hypoxia-pretreated and nontreated cardiomyocytes under room air conditions. Even under these equivalent normoxic conditions, hypoxia-pretreated cardiomyocytes produced ATP faster than nontreated control cardiomyocytes (Fig. 5*C* and Fig. S7*B*). G0s2 knockdown attenuated this increase in the rate of ATP production, indicating that the enhanced ATP production rate resulting from hypoxia pretreatment primarily depends on endogenous G0s2 induction. This increased G0s2 expression was essential for cell survival, because G0s2-depleted cells died earlier than control cells under conditions of hypoxic stress (Fig. 5*D*)

Furthermore, to assess the effect of G0s2 on cellular respiration, we continuously measured the oxygen consumption rate (OCR) using an XF96 Extracellular Flux Analyzer. G0s2 knockdown decreased the basal OCR of cardiomyocytes, most likely because of the decreased activity of ATP synthesis (Fig. 5 *E* and *F*). In contrast, the proton leakage of the mitochondrial inner membrane and the maximum respiratory capacity of OXPHOS complexes I–IV were unaffected by G0s2 ablation (Fig. 5 *E* and *F*). These data show that G0s2 knockdown reduced respiration caused by ATP synthesis without affecting respiration caused by proton leakage, nonmitochondrial respiration, or the maximal respiration capacity.

All these findings indicate that G0s2 enhances the mitochondrial ATP production rate by increasing the activity of F_oF_1-ATP synthase.

Discussion

In this study, we showed that G0s2 kinetically increased OXPHOS activity through direct binding to F_oF_1-ATP synthase. Our previous

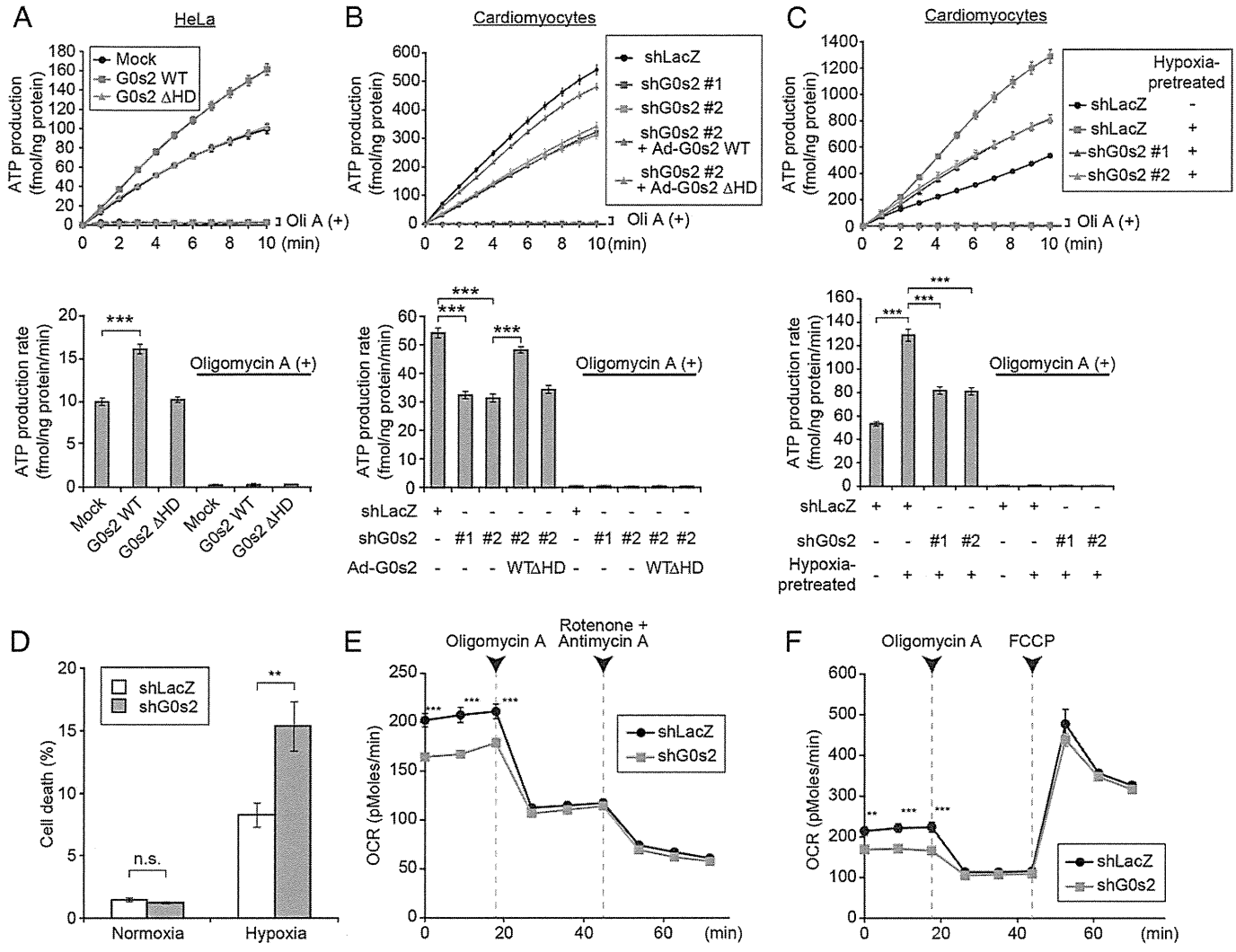

Fig. 5. G0s2 enhances the mitochondrial ATP production rate. (*A* and *B*) MASC assay of (*A*) permeabilized HeLa cells expressing the indicated plasmids or (*B*) cardiomyocytes expressing the indicated adenovirus in the presence (dotted lines) or absence (solid lines) of 1 μg/mL oligomycin A (Oli A). *Upper* shows the ATP production plots, and *Lower* shows the mean ATP production rates between 0 and 10 min. (*A*) $n = 12$. (*B*) Solid lines, $n = 12$; dotted lines, $n = 8$. (*C*) MASC assay of permeabilized cardiomyocytes pretreated with hypoxia. Cells expressing the indicated adenovirus were pretreated with or without hypoxia for 4 h. After the pretreatment, the cells were permeabilized under room air conditions followed by MASC assay in the presence (dotted lines; $n = 8$) or absence (solid lines; $n = 12$) of 1 μg/mL Oli A. *Upper* shows the ATP production plot, and *Lower* shows the mean ATP production rate between 0 and 10 min. (*D*) The bar graph represents the cell viability of G0s2-depleted cardiomyocytes under hypoxic conditions. Cardiomyocytes expressing shLacZ or shG0s2 (#2) were cultured under normoxic or hypoxic conditions for 18 h. (*E* and *F*) The OCR in cardiomyocytes expressing shLacZ and shG0s2 (#2) under basal conditions and in response to the indicated mitochondrial inhibitors ($n = 8$). FCCP, carbonyl cyanide-4-(trifluoromethoxy)-phenylhydrazone. Data are represented as the means ± SEMs. n.s., not significant. $^{**}P < 0.01$; $^{***}P < 0.001$.

studies of F_oF_1-ATP synthase have revealed that this enzyme has a specific structure that connects two molecular nanomotors that synchronize with each other to produce ATP (26–30). These physically distinct structures suggest that a specific activating factor for F_oF_1-ATP synthase must exist. Combined with the findings from this study, we hypothesize that G0s2 may lower the activation barrier of the F_oF_1-ATP synthase nanomotor and enhance the ATP production rate with the equivalent proton motive driving force (PMF; i.e., the sum of the membrane potential and the pH gradient). Activation barriers might be generated by various factors, such as friction between the stator and rotor of F_oF_1-ATP synthase, physical and electrical resistance to proton transport through the channel, and the existence of rotary blockers such as the bacterial ε-subunit and cyclophilin D (31). The increased ATP production rate caused by G0s2 overexpression observed in the MASC assay supports this hypothesis, because the PMF in the initial phase of this assay should be the same. If this hypothesis is true, even with reduced PMF, cells that express G0s2 should produce ATP faster than cells that express little or no G0s2. In fact, G0s2 overexpression attenuated the decline of $[ATP]_{mito}$ under hypoxic conditions that reduced the PMF. Precise real-time measurement of the PMF is currently difficult, but these hypotheses might be proven in future studies. Kinetically faster ATP production should accompany greater consumption of both O_2 and PMF; however, our results suggest that preserving ATP production is more beneficial than preserving PMF for cell viability, particularly when the O_2 supply is restricted but still exists. The transience of endogenous G0s2 expression induced by hypoxia might serve to protect tissues in the early phase of energy crisis. There may be specific mechanisms to decrease G0s2 expression under prolonged ischemia that have yet to be identified. Another possible mechanism by which G0s2 could increase the ATP production rate is that G0s2 increases the F_o-F_1 coupling efficiency of F_oF_1-ATP synthase. However, this hypothesis is less likely, because G0s2 altered the oxygen consumption rate to increase the ATP production rate. Although this uncoupling phenomenon has rarely been reported for mammalian mitochondrial F_oF_1-ATP synthase, we cannot completely eliminate the possibility that intrinsically

uncoupled F_oF_1-ATP synthase exists, because we could not accurately measure the amount of uncoupled F_oF_1-ATP synthase in intact cells.

G0s2 was first identified in cultured monocytes during the drug-induced cell cycle transition from G0 to G1 phase (18, 32). A limited number of studies have implied that G0s2 is involved in cell proliferation (33), differentiation (19), apoptosis (34), inflammation (35), and lipid metabolism (36) in various cellular settings. Moreover, G0s2 was reported to localize to the cytosol (33), endoplasmic reticulum (19), mitochondria (34), or the surface of lipid droplets (36). How G0s2 distinguishes these multiple functions is still not clear. In our hands, G0s2 is always localized to mitochondria, which was shown by immunostaining with two antibodies against different epitopes of G0s2 (Fig. S6). Complete depletion of mitochondrial staining by G0s2 knockdown strongly suggests the specific localization of G0s2 to mitochondria. We also showed that G0s2 specifically bound to mitochondrial F_oF_1-ATP synthase but not other OXPHOS protein complexes and functionally regulated OXPHOS activity. Together, these data suggest that G0s2 acts in the mitochondria. However, different cellular conditions may change the localization and role of G0s2. Additionally, G0s2-mediated changes in ATP metabolism may possibly affect the lipid metabolism or cellular proliferation. Additional studies will reveal the functional mechanisms by which G0s2 exerts these multiple functions in different cellular conditions.

In this study, we evaluated $[ATP]_{mito}$ and $[ATP]_{cyto}$ separately using FRET-based ATP biosensors in living cells. This dual evaluation revealed that $[ATP]_{mito}$ reflected mitochondrial ATP production with much greater sensitivity than $[ATP]_{cyto}$ (Fig. 1 and Movies S1 and S2). Because $[ATP]_{cyto}$ is strongly influenced by the activity of various cytosolic ATP hydrolytic enzymes and ATP buffering enzymes, $[ATP]_{cyto}$ does not always reflect the ATP availability that determines cellular function.

Taken together, our results indicate that G0s2 is a positive regulator of OXPHOS that works to increase the mitochondrial ATP production rate even under hypoxic conditions. Therefore, enhancing the level and function of G0s2 could be beneficial for hypoxia- and mitochondria-related disorders, such as ischemic diseases, metabolic diseases, and cancer.

Materials and Methods

Cells were infected with adenovirus encoding FRET-based ATP indicators AT1.03 or mit-AT1.03 to measure changes in cytosolic or mitochondrial ATP concentrations, respectively. Image acquisitions and FRET analyses were performed as described previously with some modifications (13). For the control of oxygen concentration during time-lapse imaging, digital gas mixer for stage-top incubator GM8000 (Tokai Hit) was used to create hypoxic (1% O_2) or normoxic (20% O_2) condition. Additional methods are found in *SI Materials and Methods*.

ACKNOWLEDGMENTS. We thank M. Murata for helpful discussions and advice, H. Miyagi (Olympus Co. Ltd.) for technical advice regarding microscopy, T. Miyazaki (Cyclex Co. Ltd.) for making antibodies, S. Ikezawa and A. Ogai for technical assistance, K. Tanaka for help with the purification of bovine F_oF_1-ATP synthase, and Y. Okada and H. Fujii for secretarial support. This research was supported by the Japan Society for the Promotion of Science through the Funding Program for Next Generation World-Leading Researchers (NEXT Program) initiated by the Council for Science and Technology Policy; grants-in-aid from the Ministry of Health, Labor, and Welfare–Japan; and grants-in-aid from the Ministry of Education, Culture, Sports, Science, and Technology–Japan. This research was also supported by grants from Takeda Science Foundation, Japan Heart Foundation, Japan Cardiovascular Research Foundation, Japan Intractable Diseases Research Foundation, Japan Foundation of Applied Enzymology, Japan Medical Association, Uehara Memorial Foundation, Mochida Memorial Foundation, Banyu Foundation, Naito Foundation, Inoue Foundation for Science, Osaka Medical Research foundation for Intractable Diseases, Ichiro Kanehara Foundation, and Showa Houkoukai.

1. Kim JW, Tchernyshyov I, Semenza GL, Dang CV (2006) HIF-1-mediated expression of pyruvate dehydrogenase kinase: A metabolic switch required for cellular adaptation to hypoxia. *Cell Metab* 3(3):177–185.
2. Papandreou I, Cairns RA, Fontana L, Lim AL, Denko NC (2006) HIF-1 mediates adaptation to hypoxia by actively downregulating mitochondrial oxygen consumption. *Cell Metab* 3(3): 187–197.
3. Semenza GL (2012) Hypoxia-inducible factors in physiology and medicine. *Cell* 148(3): 399–408.
4. Semenza GL, et al. (1996) Hypoxia response elements in the aldolase A, enolase 1, and lactate dehydrogenase A gene promoters contain essential binding sites for hypoxia-inducible factor 1. *J Biol Chem* 271(51):32529–32537.
5. Chen YC, et al. (2012) Identification of a protein mediating respiratory supercomplex stability. *Cell Metab* 15(3):348–360.
6. Fukuda R, et al. (2007) HIF-1 regulates cytochrome oxidase subunits to optimize efficiency of respiration in hypoxic cells. *Cell* 129(1):111–122.
7. Strogolova V, Furness A, Robb-McGrath M, Garlich J, Stuart RA (2012) Rcf1 and Rcf2, members of the hypoxia-induced gene 1 protein family, are critical components of the mitochondrial cytochrome bc1-cytochrome c oxidase supercomplex. *Mol Cell Biol* 32(8):1363–1373.
8. Saks V, et al. (2006) Cardiac system bioenergetics: Metabolic basis of the Frank-Starling law. *J Physiol* 571(Pt 2):253–273.
9. Smolenski RT, Lachno DR, Ledingham SJ, Yacoub MH (1990) Determination of sixteen nucleotides, nucleosides and bases using high-performance liquid chromatography and its application to the study of purine metabolism in hearts for transplantation. *J Chromatogr A* 527(2):414–420.
10. Shimura D, et al. (2013) Metabolomic profiling analysis reveals chamber-dependent metabolite patterns in the mouse heart. *Am J Physiol Heart Circ Physiol* 305(4):H494–H505.
11. Kemp GJ, Meyerspeer M, Moser E (2007) Absolute quantification of phosphorus metabolite concentrations in human muscle in vivo by 31P MRS: A quantitative review. *NMR Biomed* 20(6):555–565.
12. Ford SR, et al. (1996) Use of firefly luciferase for ATP measurement: Other nucleotides enhance turnover. *J Biolumin Chemilumin* 11(3):149–167.
13. Imamura H, et al. (2009) Visualization of ATP levels inside single living cells with fluorescence resonance energy transfer-based genetically encoded indicators. *Proc Natl Acad Sci USA* 106(37):15651–15656.
14. Lopaschuk GD, Kelly DP (2008) Signalling in cardiac metabolism. *Cardiovasc Res* 79(2): 205–207.
15. Hattori F, et al. (2010) Nongenetic method for purifying stem cell-derived cardiomyocytes. *Nat Methods* 7(1):61–66.
16. Forsythe JA, et al. (1996) Activation of vascular endothelial growth factor gene transcription by hypoxia-inducible factor 1. *Mol Cell Biol* 16(9):4604–4613.
17. Wolf A, et al. (2011) Hexokinase 2 is a key mediator of aerobic glycolysis and promotes tumor growth in human glioblastoma multiforme. *J Exp Med* 208(2):313–326.
18. Russell L, Forsdyke DR (1991) A human putative lymphocyte G0/G1 switch gene containing a CpG-rich island encodes a small basic protein with the potential to be phosphorylated. *DNA Cell Biol* 10(8):581–591.
19. Zandbergen F, et al. (2005) The G0/G1 switch gene 2 is a novel PPAR target gene. *Biochem J* 392(Pt 2):313–324.
20. Heckmann BL, Zhang X, Xie X, Liu J (2013) The G0/G1 switch gene 2 (G0S2): Regulating metabolism and beyond. *Biochim Biophys Acta* 1831(2):276–281.
21. Dimroth P, von Ballmoos C, Meier T (2006) Catalytic and mechanical cycles in F-ATP synthases. Fourth in the Cycles Review Series. *EMBO Rep* 7(3):276–282.
22. Senior AE (2007) ATP synthase: Motoring to the finish line. *Cell* 130(2):220–221.
23. Walker JE (1998) ATP synthesis by rotary catalysis (Nobel Lecture). *Angew Chem Int Ed* 37:5000–5011.
24. Yoshida M, Muneyuki E, Hisabori T (2001) ATP synthase—a marvellous rotary engine of the cell. *Nat Rev Mol Cell Biol* 2(9):669–677.
25. Fujikawa M, Yoshida M (2010) A sensitive, simple assay of mitochondrial ATP synthesis of cultured mammalian cells suitable for high-throughput analysis. *Biochem Biophys Res Commun* 401(4):538–543.
26. Adachi K, et al. (2007) Coupling of rotation and catalysis in F(1)-ATPase revealed by single-molecule imaging and manipulation. *Cell* 130(2):309–321.
27. Itoh H, et al. (2004) Mechanically driven ATP synthesis by F1-ATPase. *Nature* 427(6973):465–468.
28. Noji H, Yasuda R, Yoshida M, Kinosita K, Jr. (1997) Direct observation of the rotation of F1-ATPase. *Nature* 386(6622):299–302.
29. Rondelez Y, et al. (2005) Highly coupled ATP synthesis by F1-ATPase single molecules. *Nature* 433(7027):773–777.
30. Uchihashi T, Iino R, Ando T, Noji H (2011) High-speed atomic force microscopy reveals rotary catalysis of rotorless F_1-ATPase. *Science* 333(6043):755–758.
31. Giorgio V, et al. (2009) Cyclophilin D modulates mitochondrial F0F1-ATP synthase by interacting with the lateral stalk of the complex. *J Biol Chem* 284(49):33982–33988.
32. Siderovski DP, Blum S, Forsdyke RE, Forsdyke DR (1990) A set of human putative lymphocyte G0/G1 switch genes includes genes homologous to rodent cytokine and zinc finger protein-encoding genes. *DNA Cell Biol* 9(8):579–587.
33. Yamada T, Park CS, Burns A, Nakada D, Lacorazza HD (2012) The cytosolic protein G0S2 maintains quiescence in hematopoietic stem cells. *PLoS ONE* 7(5):e38280.
34. Welch C, et al. (2009) Identification of a protein, G0S2, that lacks Bcl-2 homology domains and interacts with and antagonizes Bcl-2. *Cancer Res* 69(17):6782–6789.
35. Kobayashi S, et al. (2008) Expression profiling of PBMC-based diagnostic gene markers isolated from vasculitis patients. *DNA Res* 15(4):253–265.
36. Yang X, et al. (2010) The G(0)/G(1) switch gene 2 regulates adipose lipolysis through association with adipose triglyceride lipase. *Cell Metab* 11(3):194–205.